Colloids and Surfaces A: Physicochem. Eng. Aspects 449 (2014) 31–41

Contents lists available at ScienceDirect

Colloids and Surfaces A: Physicochemical and Engineering Aspects

journal homepage: www.elsevier.com/locate/colsurfa

Modification of silicon oxide surfaces by monolayers of an oligoethylene glycol-terminated perfluoroalkyl silane

Frank Meiners[a], Jan Henning Ross[a], Izabella Brand[a], Anna Buling[b,1], Manfred Neumann[b], Philipp Julian Köster[c], Jens Christoffers[a], Gunther Wittstock[a,*]

[a] Carl von Ossietzky University of Oldenburg, School of Mathematics and Science, Center of Interface Science, Department of Chemistry, D-26111 Oldenburg, Germany
[b] University of Osnabrück, Department of Physics, D-49069 Osnabrück, Germany
[c] University of Rostock, Department of Biophysics, D-18057 Rostock, Germany

HIGHLIGHTS

- A new oligoethylene gylcol-terminated perfluorinated silane was synthesized.
- The hybrid silane self-assemblies on silica surfaces to form mono- or multilayers.
- The molecular-scale order in films depends on the topography of the substrate.
- Slow kinetics of the silane lattice polymerization result in a monolayer formation.

GRAPHICAL ABSTRACT

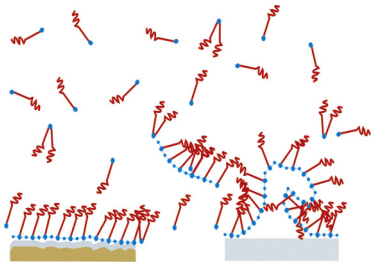

ARTICLE INFO

Article history:
Received 18 December 2013
Received in revised form 4 February 2014
Accepted 5 February 2014
Available online 22 February 2014

Keywords:
Self-assembled monolayer
Silicon oxide surface
Oligoethylene glycol
Perfluorinated silane
Hybrid molecule
Scanning force microscopy

ABSTRACT

Monolayers of a new hybrid compound having two linearly coupled subunits with different functionalities were prepared on the silicon oxide and silicate-like surfaces using trichlorosilane as an anchoring group. The two subunits of the hybrid compound are a perfluorinated alkyl chain and an oligoethylene glycol chain. The synthesis of the new precursor compound, *O*-methyl hexaethylene glycol-icosafluorododecandiol-trichlorosilane is reported starting from commercially available triethylene glycol and perfluorododecan-1,12-diol as building blocks. The final and intermediate products were characterized by nuclear magnetic resonance (^{1}H NMR, ^{13}C NMR, ^{19}F NMR and ^{29}Si NMR), infrared spectroscopy (IR) and high resolution mass spectrometry with chemical ionization [HRMS (CI)]. The new compound was self-assembled on borosilicate glass, surface-oxidized silicon and silicon oxide surfaces. Properties of the self-assembled films as a function of the adsorption time were studied using contact angle measurements, X-ray photoelectron spectroscopy, polarization modulation infrared reflection absorption spectroscopy and scanning force microscopy. The adsorption of the hybrid silane on an atomically flat silica surface lead to the formation of poorly defined multilayer films. By contrast, the adsorption of the silane onto a less-ordered substrate resulted in the formation of a well-packed monolayer.

* Corresponding author. Tel.: +49 441 798 3971; fax: +49 441 798 3684.
E-mail addresses: f.meiners@uni-oldenburg.de (F. Meiners), jan.h.ross@gmx.de (J.H. Ross), izabella.zawisza@uni-oldenburg.de (I. Brand), a.buling@hs-osnabrueck.de (A. Buling), mneumann@uos.de (M. Neumann), philipp.koester@uni-rostock.de (P.J. Köster), jens.christoffers@uni-oldenburg.de (J. Christoffers), gunther.wittstock@uni-oldenburg.de (G. Wittstock).
[1] Present address: University Applied Sciences Osnabrück, School of Engineering and Informatics, Laboratory of Material Design and Material Reliability and Laboratory for Process Engineering, Albrechtstrasse 30, D-49076 Osnabrück, Germany.

http://dx.doi.org/10.1016/j.colsurfa.2014.02.015
0927-7757/

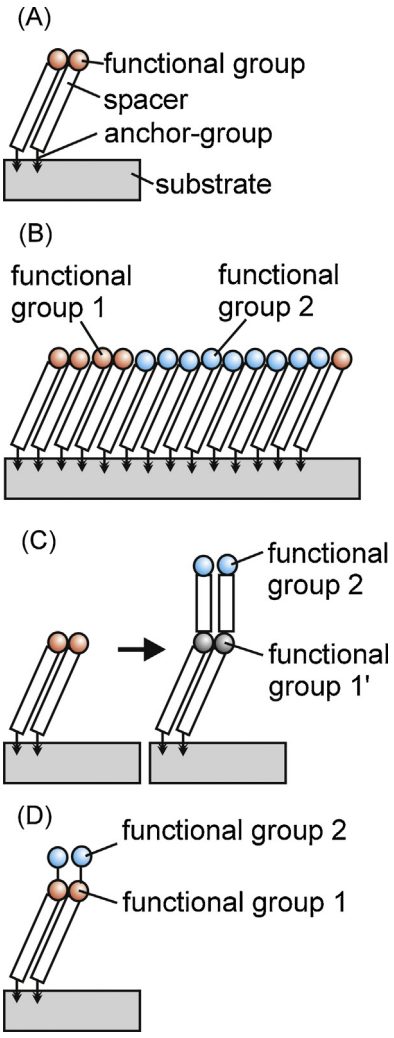

Scheme 1. Schematic representation of various SAM systems: (A) a monolayer with one functional group (FG), (B) patterned monolayer containing two kinds of compounds with two FG at different regions, (C) sequential build-up monolayer containing two compounds with two FG and (D) monolayer formed from one molecule containing two FG.

1. Introduction

Modification of technologically interesting surfaces by self-assembled monolayers (SAM) represents one important strategy to form chemically well-defined surfaces exhibiting a particular chemical functionality (Scheme 1A). Several reviews are available for such modifications exploiting different chemistries on a number of different substrate surfaces [1–6]. SAMs with more than one functional subunit have been created as patterned monolayers. Such layers expose different functional moieties at different regions of the surface (Scheme 1B). These patterns can be obtained by introducing sequentially two kinds of SAM-forming molecules, for instance by microcontact printing and backfilling [7], local removal-refilling procedures [8,9], local transformation of functional groups of a preformed monolayer [10,11], or by formation/modification of monolayers on pre-patterned and locally addressable substrates [12]. Linearly arranged functional groups may result from sequential build-up of complex surface architectues; i.e. an initially formed reactive surface is chemically modified to obtain a more complex interfacial structure [13]. Typically, the desired function is provided by the functional unit added last to the interfacial system while the other functional groups become linking units (Scheme 1C), for instance, a SAM of triazol-linked monolayer produced via copper-catalyzed Huisgen-1,3-dipolar azide-alkyne cycloaddition (so called "Click reaction") [14]. Another approach uses the formation of SAMs from molecules containing two (or more) functional groups as shown in Scheme 1D. While molecules containing different functional groups with precisely designed properties are highly required for modification of complex surfaces, the synthesis of such systems as well as the adsorption process tend to be complicated due to possible reactivities between individual building blocks (anchor group and multiple functional groups). In this paper we report film properties of a new hybrid compound containing two functional groups (Scheme 1D). The hybrid compound contains a methoxy terminated hexaoligoethylene glycol (OEG) unit connected to a perfluorinated alkyl chain anchoring via a trichlorosilane group to the silica surface. The silane chemistry is used to chemisorb the molecule to glass and different silicon oxide (SiO_x) surfaces.

Devices fabricated of glass, silicon oxides and silicon nitrides-coated silicon surfaces find numerous applications as implant and biosensor materials [15,16], "lab-on-chips" and microfluidic chips [17,18] and assays platforms for peptide synthesis [19]. Silica nanoparticles are tested as possible drug delivery vehicles [20] or superhydropobic surface coatings [21]. In those applications, polymers are alternatives to glass and silica material of choice. Despite high costs, glass and silicon oxide remain the most favorable materials due to reproducible fabrication protocols, well understood surface chemistry and biocompatibility [17,18]. However, a non-specific adsorption of proteins as well as cell adhesion (so-called biofouling) may interfere with device performance. Chemisorption of silanes on glass and silica surfaces provides enormous possibilities of surface modifications aiming at tuning the surface properties of a device [17,22–24]. Surface modifications of glass and silicon oxide surfaces preventing non-specific protein adsorption and biofouling are of large importance for application. For this purpose protein films, polymer coatings [22,23], self-assembled monolayers [24,25] of small amphiphilic molecules and large polymer molecules [26] are commonly used. Molecules containing oligoethylene glycol (OEG) or polyethylene glycol (PEG) units provide the most frequently used coating preventing biofouling [22]. Various modifications or OEG units were tested to allow their chemisorption on gold, silver [27], glass, SiO_x [28,29], indium tin oxide (ITO) [30], oxidized silicon [31] or silicon nitride [32] surfaces.

A perfluorocarbon chain, the second functional group in the new molecule reported here, has good biocompatibility, is lipophobic and shows a high chemical and biological inertness [33,34]. A H-terminated Si(1 1 1) surface modified by a SAM of perfluorinated alkyl chains [35] has significantly reduced friction and adhesion properties. Gentilini et al. [36,37] synthesized an OEG-terminated perfluorinated thiol to passivate Au-nanoparticles. The introduction of a perfluorocarbon chain to the OEG subunit offers new possibilities of the surface modification, which may find numerous biotechnological applications. The particular challenge for the synthesis of hybrid compounds containing a perfluorocarbon chain is due to the strong electron-withdrawing effect of the F atom on the adjacent C atom, making classical nucleophilic substitutions very difficult. In this paper, we report for the first time in the literature the synthesis of a new silane analogue of the thiol reported by Gentilini et al. [36,37] and the formation of monolayers on oxidic surfaces.

2. Materials and methods

2.1. Materials

1H,1H,12H,12H-perfluorododecane-1,12-diol (**5**) (Alfa Aesar, Karlsruhe, Germany) and dichloromethane (99.9% extra dry,

Acros Organics, Nidderau, Germany) were used as received. All other starting materials and solvents were purchased from Sigma–Aldrich (Steinheim, Germany) as commercial grade and used as received. Preparative column chromatography was carried out using SiO_2 (35–70 μm, type 60 A; Merck, Darmstadt, Germany). TLC was performed on aluminum plates coated with SiO_2 F254 (Merck). Air-oxidized silicon wafers (Si/SiO_x) with a 1000 nm SiO_2-layer on a silicon wafer, Borofloat®33 (BF33) glass wafer, and gold substrates coated with a 10 nm thick layer of chemical vapor deposited silicon oxide (Au/SiO_x) were obtained from iX factory (Dortmund, Germany). Silica coating on an oxidized silicon wafer and glass (BF33) were used in order to compare the process of chemisorption of synthesized silicates at pure SiO_2 and disordered glass surfaces. Both surfaces have comparable surface roughness and they are flat at the atomic level. Au/SiO_x samples were fabricated according to earlier described procedures [38,39] in order to provide a mirror surface for polarization modulation infrared reflection absorption (PM IRRA) spectroscopy and a thin SiO_x layer for the attachment of the silanes. The surface roughness of Au/SiO_x surface is close to 1.0 nm and is higher than the surface roughness of the two other materials.

2.2. Instrumentation

Nuclear magnetic resonance spectra were obtained in $CDCl_3$ at 23 °C with a Bruker Avance DRX 500 instrument (500 MHz for ^1H, 125 MHz for ^{13}C, 470 MHz for ^{19}F, and 100 MHz for ^{29}Si). Multiplicities of carbon signals were determined with distorsionless enhancement by polarization transfer (DEPT) experiments. Infrared spectra were recorded on a Bruker Tensor 27 spectrometer equipped with a "GoldenGate" diamond attenuated total reflection (ATR) unit. High resolution mass spectra (HRMS) were obtained with a Finnigan MAT 95 (CI) spectrometer.

The static water contact angle was measured by the sessile drop method using 2 μL drops of deionized water with the contact angle system OCA 15plus (DataPhysics, Filderstadt, Germany) equipped with a CCD camera and the SCA20 software (version 1.0.0). The quoted values are the average of three measurements on different freshly modified and cleaned samples of Au/SiO_x and BF33 glass wafers.

Modified Si/SiO_x and BF33 surfaces were cleaned as described in Section 2.3.3 and imaged by scanning force microscopy (SFM) in the Tapping mode™ using a Nanoscope IIIA controller, a Dimension 3100 sample stage and scanner and a TESP tip with a nominal force constant of 42 N m^{-1} (all Veeco Instruments Inc., Plainview, NY, USA). The measurement of the modified Au/SiO_x surfaces were obtained in the contact mode in water using an Enviroscope with a Enviroscope controller (all Veeco Instruments Inc., Plainview, NY, USA) and a MSCT tip with a nominal force constant of 0.03 N m^{-1} and a resonant frequency of 10–20 kHz (Bruker Corporation, Billerica, MA, USA). Images of 256 × 256 pixel within 1 μm × 1 μm and 5 μm × 5 μm areas were recorded with a scan rate of 1 Hz. Images are shown after background subtraction ("Flattening") using a first order polynomial using the Nanoscope software (V5.30r3sr3). Root mean square (RMS) values were determined with this software on a 5 μm × 5 μm region.

X-ray photoelectron (XP) spectra (XPS) were recorded using a PHI 5600ci multitechnique spectrometer (Physical Electronics, Chanhassen, MN, USA) with monochromatic Al Kα radiation ($h\nu$ = 1486.6 eV) of 0.3 eV FWHM bandwidth. The pass energy of the monochromator was set to 29 eV for the high-resolution spectra yielding a resolution of 0.44 eV. All spectra were obtained using a 400 μm diameter analysis area. During the measurements, the pressure in the main chamber was kept at about 10^{-9} mbar. The spectra were referenced to the Si 2p peak of SiO_2 centered at 103.3 eV [40]. Spectra were analyzed using the XPSPeak software (version 4.1). Measured XP spectra are shown as filled circles, the background and the spectral components are thin solid line and the fitted spectrum is a thick solid line.

PM IRRA spectra were measured with a Vertex 70 spectrometer and an external reflection setup (Bruker, Ettlingen, Germany) containing a photoelastic modulator (PEM) PMA 50 (Hinds Instruments, Hillsboro, OR, USA). The resolution of the recorded spectra was 4 cm^{-1}. The half-wave retardation (i.e. the maximum PEM efficiency) was set at 2900 cm^{-1} for the analysis of the CH-stretching modes and at 1100 cm^{-1} for the analysis of the SiO_2 and CF_2 stretching modes. The incident angle was 80°. The spectra were Min/Max normalized using the OPUS software (version 5.5, Bruker). This method scales the intensity values that the minimum is set to zero absorption units and the maximum intensity to two absorption units.

2.3. Procedures

The synthesis of compound **7**, the precursor for SAM formation, is depicted in Scheme 2 and started from commercially available triethylene glycol monomethyl ether (**1**). It will be discussed in detail in the next section.

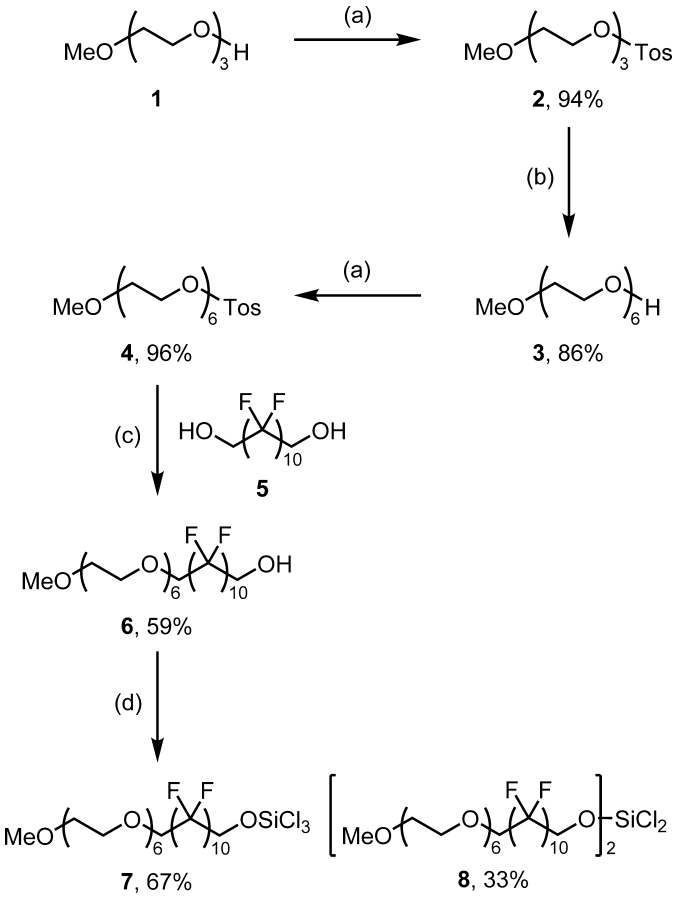

Scheme 2. Preparation of monolayer-precursor **7**. Reagents and conditions: (a) 2 equiv. TosCl, 2 equiv. NEt_3, CH_2Cl_2, 23 °C, 2.5 h (for **1**) or 18 h (for **3**); (b) 5.3 equiv. triethylene glycol, 3.1 equiv. KOH, 100 °C, 18 h; (c) 2 equiv. $HOCH_2(CF_2)_{10}CH_2OH$ (**5**), 1.4 equiv. NaH, THF, 23 °C, 45 min; then adding tosylate **4**, 80 °C, 4 h; (d) xs. $SiCl_4$, 70 °C, 1 h; then high vacuum. Tos = 4-$MeC_6H_4SO_2$.

2.3.1. Preparation of 22,22,23,23,24,24,25,25,26,26,27,27,28,28,29,29,30,30,31,31-icosafluoro-2,5,8,11,14,17,20-heptoxadotriacontan-32-ol (6)

NaH (60% dispersion in mineral oil, 102 mg, 2.55 mmol) was added under exclusion of air and moisture (N_2 atmosphere) to a solution of perfluorodiol (**5**; 2.00 g, 3.56 mmol) in abs. THF (30 mL) and the resulting suspension was stirred for 45 min at ambient temperature. Then tosylate (**4**; 0.80 g, 1.78 mmol) was added and the mixture further heated to reflux for 4 h. It was then diluted with CH_2Cl_2 (30 mL) and brine (30 mL) and the layers were separated. The organic layer was washed with H_2O (20 mL) and the combined aqueous phases was reextracted twice with CH_2Cl_2 (2 mL × 20 mL). The combined organic layers were dried ($MgSO_4$) and evaporated after filtration. The residue was submitted to column chromatography [SiO_2, EtOAc/MeOH 19: 1 (v/v)]. The first fraction (R_f = 0.78) contained diol **5** (630 mg, 1.12 mmol, 31%) as a colorless solid. Secondly, the title compound (**6**; 878 mg, 1.04 mmol, 59%; R_f = 0.47, colorless oil) was eluted. ^{1}H NMR (500 MHz, $CDCl_3$): δ = 3.34 (s, 3 H), 3.49–3.53 (m, 2 H), 3.58–3.66 (m, 20 H), 3.73–3.76 (m, 2 H), 3.95–4.07 (m, 4 H) ppm. $^{13}C\{^1H\}$ NMR (125 MHz, $CDCl_3$): δ = 58.80 (CH_3), 60.17 (*t*, *J* = 25.1 Hz, $CF_2\underline{C}H_2$), 68.20 (*t*, *J* = 25.3 Hz, $CF_2\underline{C}H_2$), 70.36 (CH_2), 70.44 (3 CH_2), 70.45 (3 CH_2), 70.47 (CH_2), 70.53 (CH_2), 70.61 (CH_2), 71.82 (CH_2), 72.22 (CH_2), 108.03–109.51 (m, 2 CF_2), 110.44–111.64 (m, 4 CF_2), 112.43–114.11 (m, 2 CF_2), 115.17–116.19 (m, CF_2), 117.28–118.15 (m, CF_2) ppm. $^{19}F\{^1H\}$ NMR (470 MHz, $CDCl_3$): δ = (−123.57)–(−123.32) (m, 4 F), (−122.32)–(−122.16) (m, 2 F), (−122.05)–(−121.84) (m, 4 F), (−121.84)–(−121.54) (m, 8 F), (−119.79)–(−119.62) (m, 2 F) ppm. IR (ATR): λ^{-1} = 3406 (w, br.), 2877 (w, br.), 1456 (w), 1351 (w), 1200 (s), 1135 (vs), 943 (m), 850 (m), 708 (m), 653 (m) cm^{-1}. HRMS (CI, isobutane): calcd. 841.1856 (for $C_{25}H_{33}F_{20}O_8$); found 841.1861 [M + H^+]. $C_{25}H_{32}F_{20}O_8$ (840.48).

2.3.2. Preparation of 1,1,1-trichloro-4,4,5,5,6,6,7,7,8,8,9,9,10,10,11,11,12,12,13,13-icosafluoro-2,15,18,21,24,27,30,33-octoxa-1-silatetriacontane (7)

While cooling with an ice-water bath, alcohol (**6**; 105 mg, 0.12 mmol) was added under exclusion of air and moisture (N_2 atmosphere) to $SiCl_4$ (1.5 mL, 13.1 mmol). The resulting mixture was stirred for 1 h at 70 °C. Then all volatile materials (HCl and $SiCl_4$) were removed in high vacuum to yield a colorless oil, which consisted of 67% of compound **7** and 33% of byproduct **8** (molar fractions according to integration of the ^{1}H NMR spectrum). In order to obtain a stock solution for monolayer formation, the material was dissolved in abs. CH_2Cl_2 (*c* = 0.1 mol/L). Compound **7**: ^{1}H NMR (500 MHz, $CDCl_3$): δ = 3.36 (s, 3 H), 3.51–3.54 (m, 2 H), 3.60–3.67 (m, 20 H), 3.74–3.78 (m, 2 H), 4.02 (*t*, *J* = 14.0 Hz, 2 H), 4.40 (*t*, *J* = 12.9 Hz, 2 H) ppm. $^{13}C\{^1H\}$ NMR (125 MHz, $CDCl_3$): δ = 58.93 (CH_3), 62.29 (*t*, *J* = 28.6 Hz; CH_2), 68.31 (*t*, *J* = 25.3 Hz; CH_2), 70.51 (CH_2), 70.58 (5 CH_2), 70.60 (CH_2), 70.61 (CH_2), 70.67 (CH_2), 70.74 (CH_2), 71.94 (CH_2), 72.31 (CH_2), 108.27–109.73 (m, 2 CF_2), 110.20–111.76 (m, 4 CF_2), 112.54–114.39 (m, 2 CF_2), 115.25–116.36 (m, CF_2), 117.37–118.17 (m, CF_2) ppm. $^{19}F\{^1H\}$ NMR (470 MHz, $CDCl_3$): δ = (−123.68)–(−123.42) (m, 2 F), (−123.25)–(−123.08) (m, 2 F), (−122.31)–(−121.98) (m, 4 F), (−121.98)–(−121.64) (m, 8 F), (−120.94)–(−120.79) (m, 2 F), (−120.01)–(−119.76) (m, 2 F) ppm. $^{29}Si\{^1H\}$ NMR (100 MHz, $CDCl_3$): δ = −35.4 ppm. $C_{25}H_{31}Cl_3F_{20}O_8Si$ (973.92). Compound **8**: ^{1}H NMR (500 MHz, $CDCl_3$): δ = 4.36 (*t*, *J* = 12.6 Hz, 2 H) ppm, all other signals are isochronic with compound **7**. $^{13}C\{^1H\}$ NMR (125 MHz, $CDCl_3$): δ = 62.06 (*t*, *J* = 31.5 Hz, CH_2) ppm, all other signals are isochronic with compound **7**. $^{19}F\{^1H\}$ NMR (470 MHz, $CDCl_3$): δ = (−121.22)–(−121.08) (m, 2 F) ppm, all other signals are isochronic with compound **7**. $^{29}Si\{^1H\}$ NMR (100 MHz, $CDCl_3$): δ = −53.08 ppm.

2.4. Monolayer formation

Si/SiO_x, Au/SiO_x or BF33 substrates (1.5 cm × 1.5 cm) were cleaned sequentially for 5 min with toluene and isopropanol in an ultrasonic bath and dried in an Ar stream followed by oxidation in an UV/ozone cleaner (BioForce Nanosciences, Inc., Ames, IA, USA) for 30 min in order to create a hydrophilic surface. The clean oxidized surfaces were immersed in 10–15.5 mM solution of the mixture of silanes **7** and **8** (3:2) in absolute CH_2Cl_2 under Ar atmosphere for self-assembly. Depending on the used substrate, the time of the self-assembly process varied from 1 min to 48 h. The substrates were removed from the solution and then rinsed with toluene and cleaned with CH_2Cl_2 and isopropanol in an ultrasonic bath and dried in an Ar stream.

3. Results and discussion

3.1. Organic synthesis

Intermediate products **3** and **4** were reported in literature before [36]. Nevertheless, we have developed an economical and high-yield access of compound **3** starting from readily available triethylene glycol monomethyl ether (**1**), which was first tosylated to give sulfonate **2** (94% yield, Scheme 2) and then converted with triethylene glycol to furnish hexamer **3** (86% yield). Another tosylation gave compound **4** (96%). Thus, the overall yield of this three-step sequence was 79%. Similar to the report of Gentilini et al. [36], who have prepared a corresponding thiol with perfluoroalkyl and oligoethylene glycol subunits, tosylate **4** was converted with an excess of perfluorodiol **5** to obtain the hybrid compound **6**, however, the yield remained moderate (59%). This is mainly attributed to the electron withdrawing effect of the perfluorinated moiety which lowers significantly the nucleophilicity of the corresponding alcoholate in the S_N2-type displacement. Anyhow, compound **6** could be conveniently purified by column chromatography and was obtained on a reasonable scale of almost one gram. Then it was treated with an excess of neat $SiCl_4$ at elevated temperature and alcohol **6** was fully converted. After removal of all volatile materials from the reaction mixture, the residue was analyzed by NMR-spectroscopy, which revealed a composition (molar fractions) of 67% compound **7** and 33% dialkoxydichlorosilane **8**. While the major component of this mixture was unequivocally characterized by ^{1}H NMR, ^{13}C NMR, ^{19}F NMR, the minor component was identified by the diagnostic triplet at δ (^{1}H) = 4.36 ppm. The ^{29}Si NMR spectrum of the mixture showed two signals at δ (^{29}Si) = −35.4 ppm (compound **7**) and δ (^{29}Si) = −53.1 ppm (compound **8**), which were assigned by comparison with the following literature data: δ (^{29}Si) = −38.7 ppm for $EtOSiCl_3$ and δ (^{29}Si) = −56.1 ppm for $(EtO)_2SiCl_2$ [41]. We were unable to obtain mass spectra of compounds **7** and **8**. These reactive silanes cannot be separated. A mixture of **7** (67%, trichlorosilane) and **8** (33%, dichlorosilane with two alkoxy residual) was used to produce SAMs on silica surfaces. Both compounds are able to chemisorb on the silica surface. Thus, in self-assembled films both compounds **7** and **8** are present. Due to a higher concentration of compound **7** in the solution and presence of three Cl atoms which may undergo oligomerization reaction, one can expect that **7** is the main component of films self-assembled on silica surfaces. However, trichlorosilanes form the densest and best orientated monolayers, due to the formation of three Si—O—Si bonds per molecule [42–44]. According to literature a decrease in the number of chlorosubstituents for long chains a in compound **8** decreases the order of the resulting monolayers [42–44]. It also decreases the reactivity towards the surface.

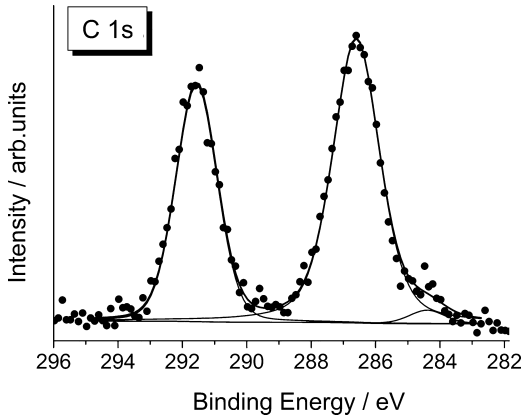

Fig. 1. C 1s high resolution XPS-spectra of **7** on the Si/SiO_x surface.

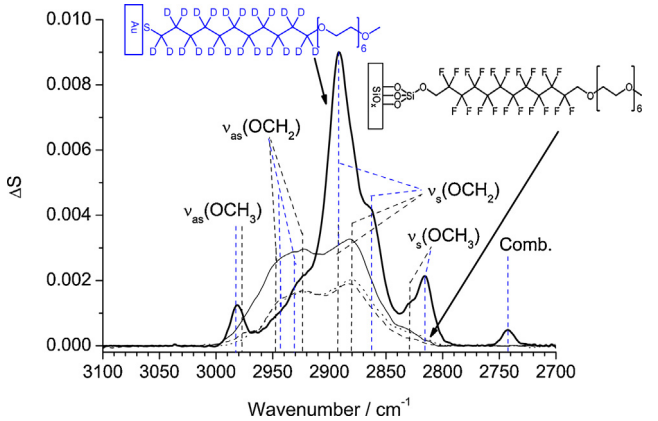

Fig. 2. PM IRRA spectra in CH stretching region of monolayers of **7** on Au/SiO_x after 3 h (dotted line), 24 h (dashed line) and 48 h (solid line) of self-assembly and PM IRRA spectrum of SAM of hexaethylene glycol-terminated per-deuterated alkanethiol adsorbed on Au (thick solid line, data are taken from [49]).

3.2. XPS-measurements of monolayers

A monolayer was formed on Si/SiO_x by immersion in a 15.5 mM solution of **7** and **8** for 3 h. The survey spectrum of the monolayer (Supporting Information, Fig. SI1) showed photoelectron signals for Si 2p, Si 2s, C 1s, O 1s and F 1s and Auger peaks of C KVV, F $KL_{23}L_{23}$, F KL_1L_{23}, O $KL_{23}L_{23}$ and O KL_1L_{23} in agreement with the elemental composition expected from the sample.

Two significant components were found in the C 1s region (Fig. 1). The first component at 286.6 eV was assigned to $\underline{C}O$ groups and corresponds to the OEG part of the monolayer [32,40]. The second line appeared at 291.6 eV and was assigned to the $\underline{C}F_2$ groups in the perfluoro alkyl chain. Moreover, a small C 1s signal at 284.4 eV was observed (Fig. 1). It was attributed to the hydrocarbon contamination (typically around 284–285 eV) [32,45]. Indeed this band was also found at the pure Si/SiO_x surface and confirms that hydrocarbon signals originated from surface contaminations.

The atomic ratio $N(\underline{C}F_2):N(\underline{C}O)$ calculated from the high resolution spectrum (Fig. 1) was 1:1.52. For compounds **7** (as well as **8**) the expected ratio $N(\underline{C}F_2):N(\underline{C}O)$ is equal to 1.0:1.5 since the hybrid compound **7** contains 10 C atoms within CF_2 groups vs. 12 C atoms in the OEG units plus 1 terminal methoxy C plus 1 C atom linking the OEG part and the perfluorinated chain and 1 C atom adjacent to the silanol group (Scheme 2). The expected and measured ratio of $N(\underline{C}F_2):N(\underline{C}O)$ were in excellent agreement indicating that indeed the hybrid compound was adsorbed on the silica surface.

One component at 688.7 eV appeared in the XPS spectrum in the F 1s region (Supporting Information, Fig. SI5). Kristalyn et al. [46] and Fréchette et al. [45] found the $C\underline{F}_2$ signal from perfluorinated silanes at 689.1 and 688.8 eV.

The O 1s region showed a broad signal at 532.9 eV (Supporting Information, Fig. SI7), which was deconvoluted into two components. The strong contribution at 533.0 eV was due to the OC at the OEG fragment [32] of **7** (as well as **8**) whereas a weak signal at 534.5 eV arose from the O atoms at SiO_x surface [40]. After removal of the monolayer of **7**, the intensity of the O 1s signal at 534.5 eV increased indicating that indeed, it originated from the silica matrix. (Supporting Information SI2, Fig. SI7).

During exposure of the monolayer of **7** to Al Kα radiation (and resulting secondary electrons), the monolayer spectra changed (Supporting Information SI2, Figs. SI2–SI7). The intensities changes under X-ray radiation did not compromise the functionalities of the layers at solid–liquid interfaces under ambient conditions.

3.3. PMIRRAS measurements

For PM IRRA measurements, a surface reflecting IR radiation is required. Therefore, Au/SiO_x substrates were used as analogues to Si/SiO_x [38]. A 10 nm thick SiO_x layer provided the OH groups for the chemisorption of silane hybrid compounds while underlying Au served as mirror for the IR radiation. Fig. 2 shows the PM IRRA spectra in the CH stretching modes region of monolayers of **7** adsorbed on the Au/SiO_x surface. Due to the presence of the perfluorinated alkane chain, the PM IRRA spectra of the CH stretching modes originated only from the OEG fragment, i.e. methylene groups adjacent to the O atoms and one terminal methoxy group. As seen in Fig. 2, the intensities of the PM IRRA spectra increased with time of self-assembly. After 48 h of the adsorption process no further changes in the PM IRRA spectra of monolayers of **7** on Au/SiO_x surface were observed. This result indicated that the monolayer formation was slow for compound **7**.

The PM IRRA spectra of SAMs of **7** were composed of several overlapped bands. A weak and poorly defined absorptions at 2976 ± 3 and $2830 \pm 5\,cm^{-1}$ arose from the $\nu_{as}(OCH_3)$ and $\nu_s(OCH_3)$ stretching modes at the terminal methoxy groups [47]. The following four IR absorption bands were assigned to the methylene stretching modes: $2949 \pm 4\,cm^{-1}$ ($\nu_{as}(OCH_2)$), $2923 \pm 2\,cm^{-1}$ ($\nu_{as}(OCH_2)$), $2892 \pm 4\,cm^{-1}$ ($\nu_s(OCH_2)$), and $2879 \pm 1\,cm^{-1}$ ($\nu_s(OCH_2)$) [47,48]. The spectra of **7** adsorbed on the Au/SiO_x surface were compared to a spectrum of a SAM of an OEG-terminated perdeuterated alkanethiol on Au [48–50] (Fig. 2). In both molecules, the OEG units were the same and, as seen in the scheme in Fig. 2, only those fragments gave absorptions in CH stretching mode region. Low intensities of the PM IRRA spectra of **7** adsorbed on Au/SiO_x in comparison to OEG-terminated alkanethiol on the Au may indicate lower surface coverage of **7** on SiO_x and/or different packing of silane and thiol molecules in the SAM.

In the CH stretching modes region, of the monolayer of **7** on the Au/SiO_x, the $\nu_s(OCH_2)$ mode at $2879\,cm^{-1}$ gave the strongest absorption band. By contrast, in monolayers of various hybrid OEG alkanethiols adsorbed on the gold, the strongest absorption originated from the $\nu_s(OCH_2)$ mode at $2890\,cm^{-1}$ [49,50]. This indicated differences in the orientation of OEG fragment in SAMs of **7** on SiO_x and its thiolate analogues on gold. The vector of the transition dipole moment of the $\nu_s(OCH_2)$ mode at $2879\,cm^{-1}$ is oriented perpendicular to the long axis of the OEG chain, whereas the transition dipole vector of the $\nu_s(OCH_2)$ mode at $2890\,cm^{-1}$ lies parallel to this axis [47]. The enhancement of the $\nu_s(OCH_2)$ mode at $2879\,cm^{-1}$ indicated that the long axis of the OEG chain had a large tilt towards the surface normal suggesting a poor packing of this part of the molecule in the self-assembled monolayer of **7** on the Au/SiO_x.

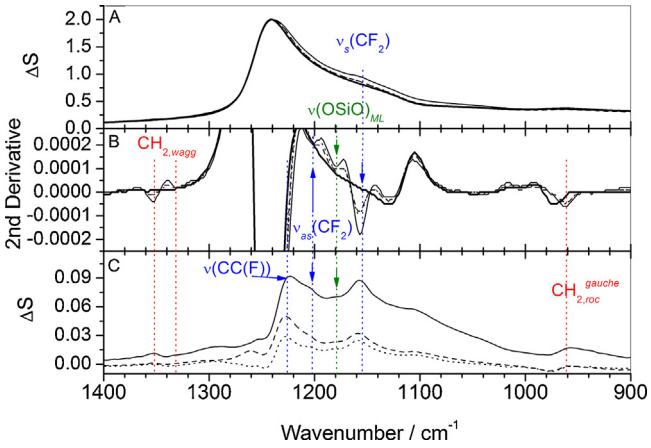

Fig. 3. Normalized PM IRRA spectra (A) and their second derivatives (B) of unmodified Au/SiO_x surface (solid line, background spectrum) and of monolayers of compound **7** on Au/SiO_x after 3 h (dotted line), 24 h (dashed line) and 48 h (thin solid line) of reaction. (C) Difference spectra of monolayers of compound **7** on Au/SiO_x and the background spectrum.

Si—O—Si modes were analyzed in the PM IRRA spectra in 1500–900 cm^{-1} region for a monolayer of **7** on the Au/SiO_x using also their second derivatives (Fig. 3).

The PM IRRA spectra were dominated by two strong, superimposed absorption bands arising from the transverse and longitudinal ν_{as}(Si—O—Si) modes in the 10 nm thick SiO_x substrate film on the Au surface (Fig. 3A) [38,51]. The hybrid compounds **7** and **8** also absorbed the IR radiation in this region complicating the analysis of the monolayer. The PM IRRA spectra of SAMs showed an increase in the intensity at 1220–1100 cm^{-1} (Fig. 3). The second derivative of the PM IRRA spectra allowed the determination of the number and frequencies of the IR absorption modes in the SAM of 7 (Fig. 3B). It had minima at 1353, 1203, 1179, 1158, 1129 and 961 cm^{-1}. In order to identify the modes originating from **7**, the PM IRRA spectra were first normalized and the difference spectrum between monolayers of compound **7** on SiO_x and the background spectrum (bare SiO_x) were calculated (Fig. 3C). The absorption at 1353 cm^{-1} originated from the CH_2 wagging modes in the amorphous, disordered phase of OEG chains [47,49]. After 24 h of the reaction, a very weak absorption around 1330 cm^{-1} appeared in the spectrum of the monolayer. The OEG part of **7** gave the CH_2 rocking mode at 961 cm^{-1}. The presence of these two modes in the PM IRRA spectra indicated that a fraction of OEG chains had gauche conformation. The presence of gauche conformations suggested that some OEG chains in the monolayer of **7** adopted a helical conformation [50,52]. Low intensities and the shape of the CH stretching modes, as well as the presence of very weak CH_2 wagging modes indicated that the OEG fragment in the monolayer of **7** existed in an amorphous state. The OEG chains were disordered and poorly packed. As shown in Fig. 3C, three absorption bands centered at 1223, 1203 and 1158 cm^{-1} originated from the CF_2 and CC(F) stretching modes of the fluorinated alkane chain of the SAM of **7** [53–55]. The mode at 1223 cm^{-1} was not resolved in the second derivative spectrum because it was superimposed on a strong absorption band of the SiO_2 substrate. This mode is due to the ν(CC(F)) stretching mode. It was found at 1226 cm^{-1} in self-assembled monolayers of perfluorinated thiols [53]. The $\nu_{as}(CF_2)$ mode was located at 1203 cm^{-1}, whereas the mode at 1158 cm^{-1} arose from the $\nu_s(CF_2)$ and $\delta(CF_2)$ modes [53,54]. A weak absorption around 1130 cm^{-1} originated from the COC stretching mode at the OEG fragment of **7** [47,50], CC progression modes in the perfluorinated chains of **7** [54] as well as Si—O—Si stretching modes in the SiO_x matrix [38]. The presence of a minimum at 1130 cm^{-1} in the second derivative of the unmodified Au/SiO_x substrate indicated that this absorption mode is due to the silica substrate. By contrast, only the second derivatives of monolayers of **7** showed a minimum at 1179 cm^{-1}. The origin of this band is not clear yet. It may arise from the asymmetric stretching mode of the O—Si—O lattice formed by **7** in the monolayer [56,57].

Table 1
Water contact angles of molecules containing a terminal OEG fragment and fluorocarbon silanes in monolayers on silica and gold surfaces.

Substrate|Adsorbed molecule	Water contact angle (°)	Reference
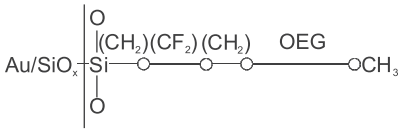	77 ± 3	This work
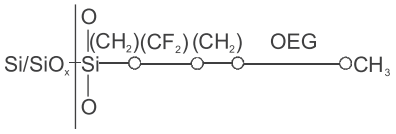	82 ± 1 81 ± 1	This work
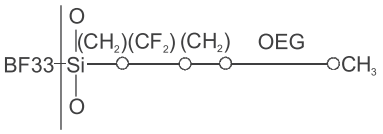		
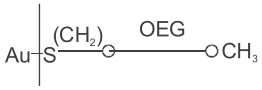	63	[46,48]
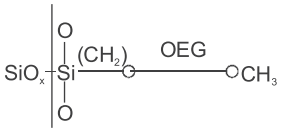	67	[24]
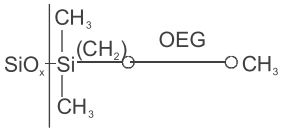	81	[25]
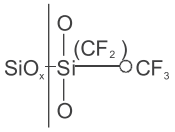	110–120	[38,42,54,55]

3.4. Contact angle measurements

After cleaning and treatment with UV/O_3, the Au/SiO_x, Si/SiO_x and BF33 surfaces were hydrophilic and their water contact angles were close to 0°. After the self-assembly of **7** on these surfaces, the water contact angle increased to ca. 80°, as listed in Table 1. The contact angle for the SAM of **7** on Au/SiO_x was equal to (77 ± 3)° and was lower than the contact angles of modified Si/SiO_x and BF33 substrates (82 ± 1)°. The measured contact angles were higher than contact angles reported for methyl-capped OEG terminated C_{11}-thiolates on gold or silver (63°) and methyl-capped-OEG-terminated-C_{11}-trichlorosilanes on SiO_x (69°) [28,50,52]. Water contact angles of monolayers of perfluorinated silanes on the SiO_x surface are higher and close to 110–120° [42,46,58,59]. Clearly, the measured water contact angles indicated that monolayers of the hybdrid compound **7** adsorbed on various silica surfaces were terminated by OEG and not by fluorocarbon chains. The value of the contact angle depends on the OEG-termination and the architecture of the whole molecule. Interestingly, Hoffmann and Tovar found

a minimum advancing contact angle of ca. 81° for SAMs formed from methyl-capped-OEG-terminated-C_{11}-dimethylchlorosilanes on silicon dioxide surfaces [29] (Table 1). Higher values of the contact angle (relative to OEG-terminated SAM on Au) reflected lower packing density and disorder in the monolayer of methyl-capped-OEG-terminated-C_{11}-dimethylchlorosilanes [29]. In our case higher values of the contact angle in monolayers of **7** compared to other OEG-terminated films indicated that the methyl capped OEG-terminated silanes are less densely packed permitting some interaction of the perfluorinated alkyl chain with water during the contact angle measurement. The observed differences were smaller for SAMs of **7** on the Au/SiO_x substrate (77° compared to 81° and 82° for SAMs on Si/SiO_x and BF33) and indicated that this SAM has a higher degree of order than films prepared on the Si/SiO_x and BF33 surfaces.

3.5. SFM-measurements

SFM images were recorded in contact mode in water for bare Au/SiO_x and Au/SiO_x modified with silane **7** (Fig. 4).

The bare Au/SiO_x surface was composed of grains which are in average 156 nm in diameter and 1–2 nm high. The surface roughness, determined as RMS over 5 μm × 5 μm surface, of the bare substrate was equal to (0.94 ± 0.04) nm. After 3 h of self-assembly of **7**, the height of features increased to 3–5 nm and the RMS increased to (1.27 ± 0.12) nm (Fig. 4B). The topography of the monolayer was dominated by the topographic features of the substrate. The uniform coating of the substrate became apparent from the lateral force images of the bare and modified Au/SiO_x samples (Fig. 4C and D). Local friction forces decreased in the monolayer of **7** chemisorbed on Au/SiO_x surface. It is known that perfluorinated silanes reduce the local friction and the adhesion due to weakening of the interaction between the AFM tip and the sample [59]. In addition, Tizazu et al. [60] reported a weaker local friction for glass substrates modified with OEG-terminated silanes compared to bare oxidized glass substrates.

Interestingly, SFM images showed large difference in topography of the monolayer of **7** prepared on the BF33 substrate (Fig. 5). The RMS of a clean 5 μm × 5 μm BF33 surface is equal to (0.267 ± 0.004) nm. The BF33 surface is very smooth and practically flat on the atomic level. Already after 1 min of the self-assembly of **7** the RMS increased to (1.157 ± 0.131) nm.

New features of a height 2.9–5.4 nm appeared on the SFM image (Fig. 5A). Longer self-assembly times caused further changes in the topography and roughness of the glass surface. In the film produced after 10 min self-assembly of **7**, the density of surface aggregates increased. The height of the features ranged from 7.2 to 13.8 nm and the RMS increased to (4.0 ± 1.0) nm. After 1 h of self-assembly, a densely packed film was formed from 1.1 nm × 0.6 nm large aggregates. Their height increased to 29.2 nm while the RMS rose to (8.07 ± 0.29) nm. Similar changes in the topography and roughness were observed for monolayers of **7** on Si/SiO_x surfaces (data not shown). The RMS of the bare Si/SiO_x surface increased from (0.463 ± 0.029) nm to (8.090 ± 0.106) nm after 4 h of self-assembly of **7**. The length of a molecule can be estimated by increments for each group. The hybrid compound **7** contains two CH_2 groups, each of it is 0.126 nm long, 10 CF_2 units each of it is 0.13 nm long, the terminal methyl group which is 0.153 nm long, and 6 ethylene glycol units of variable length. The incremental length of the ethylene glycol units depends on the chain conformation and is equal to 0.278 nm in helical and 0.356 nm in planar conformation [50]. Therefore, the expected length of the stretched molecule **7** varies from 3.373 to 3.841 nm for helical or planar conformation of the OEG chain, respectively. Therefore, the height of the observed structure exceeded the length of the hybrid molecule **7** indicating that oligomers or multilayers were formed in these regions.

Clearly, adsorption of **7** lead to the formation of non-uniform, multilayered films on BF33 and Si/SiO_x surfaces. This can be caused by the attachment of oligomers to the surface, which might be formed in solution by hydrolysis and polymerization of compound **7** and/or **8**. Such larger siloxane species might also

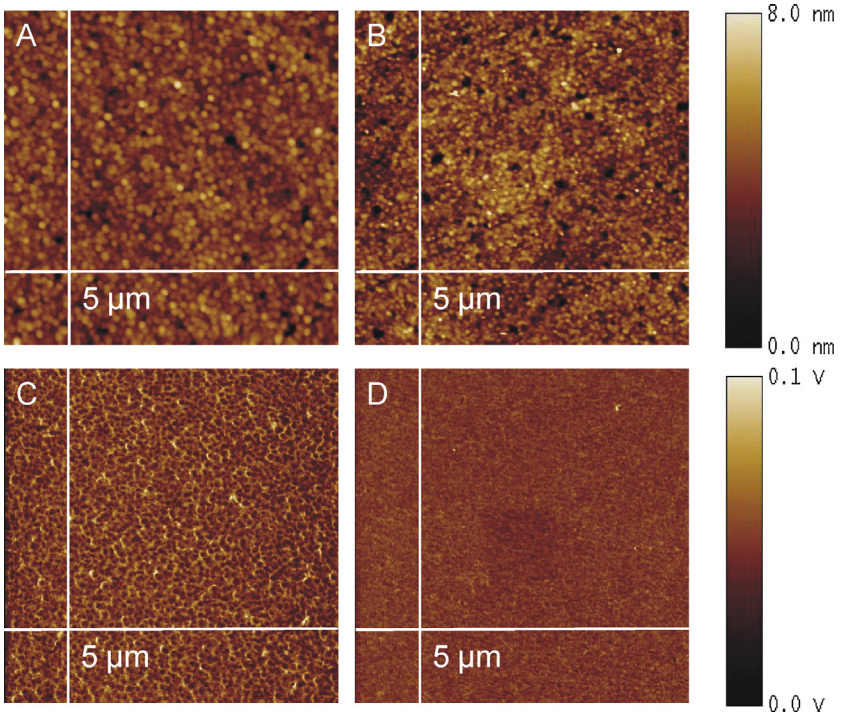

Fig. 4. SFM topography contact mode images in water of (A) bare Au/SiO_x and (B) monolayer of **7** after 3 h of self-assembly on the Au/SiO_x surface. SFM friction images with lateral force mode of (C) bare and (D) modified Au/SiO_x surface.

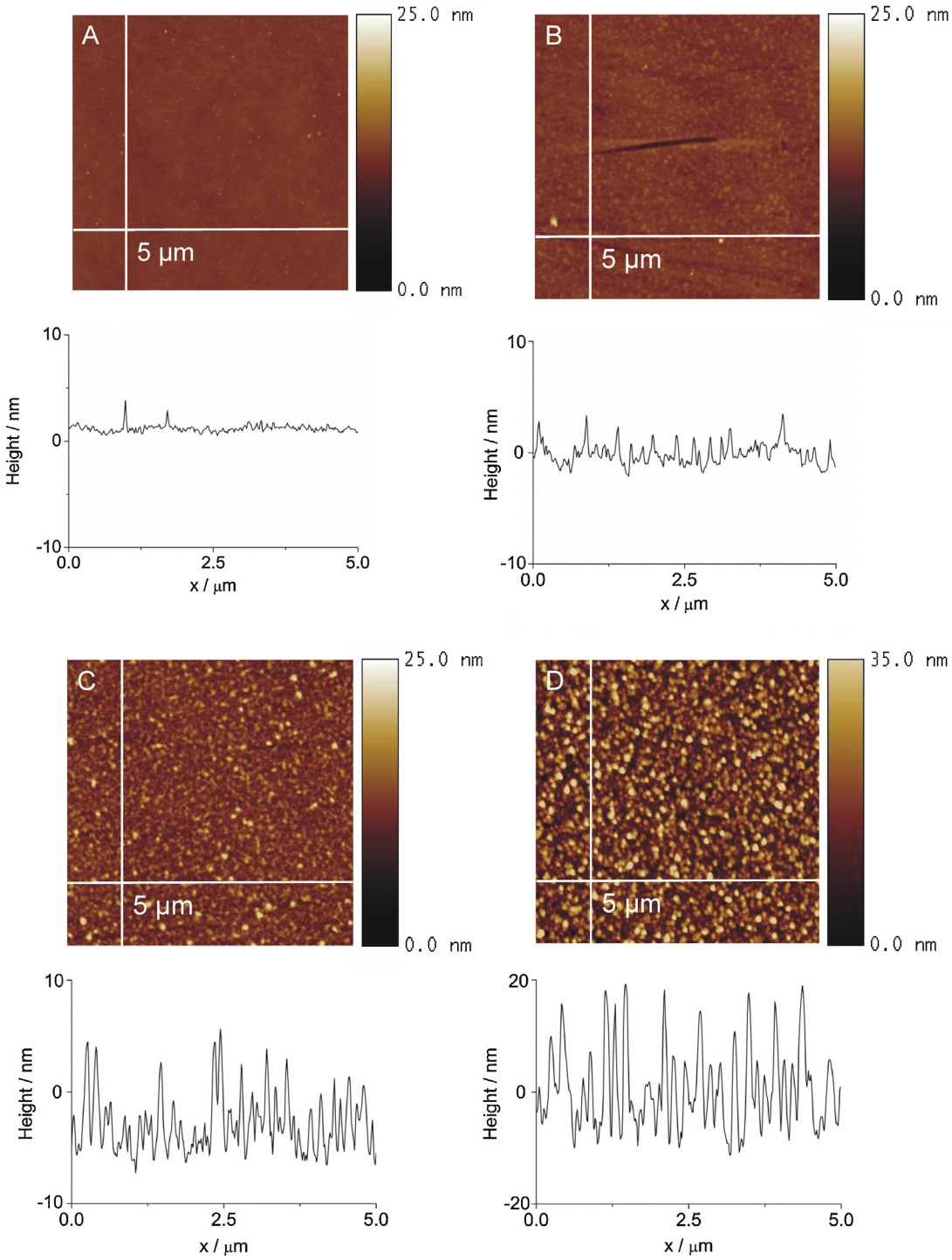

Fig. 5. Tapping mode SFM topography images and section analysis of (A) bare BF33 wafer and (B–D) BF33 surface after the self-assembly of **7** from CH_2Cl_2 solution for (B) 1, (C) 10 and (D) 60 min.

physically adsorb on solid surfaces. Bunker et al. [59] and Pellerite et al. [58] observed also that perfluorinated silanes formed aggregates on Si wafers. The size of aggregates depended on the self-assembly duration. Pellerite et al. [58] prepared a perfluorinated silane on Si wafers by immersion in heptane. The height of the used trichloro-1*H*,1*H*,2*H*,2*H*-perfluorododecylsilane adsorbed on the Si surface varied from 1.5 to 6.0 nm and 1.5 to 15.0 nm in films produced during 1 and 60 min of adsorption, respectively [58].

By contrast, the adsorption of **7** on the Au/SiO_x surface lead to the formation of well-defined monolayers. Our results suggest that the difference in the film quality was rather caused by the nature and/or surface quality of the substrate as the same conditions for cleaning and monolayer formation were applied to each sample. The BF33 samples consisted of 81% SiO_2, 2% Al_2O_3, 4% Na_2O/K_2O and 13% B_2O_3 and was atomically smooth. The Au/SiO_x surface is composed of grains and is not smooth on the atomic level.

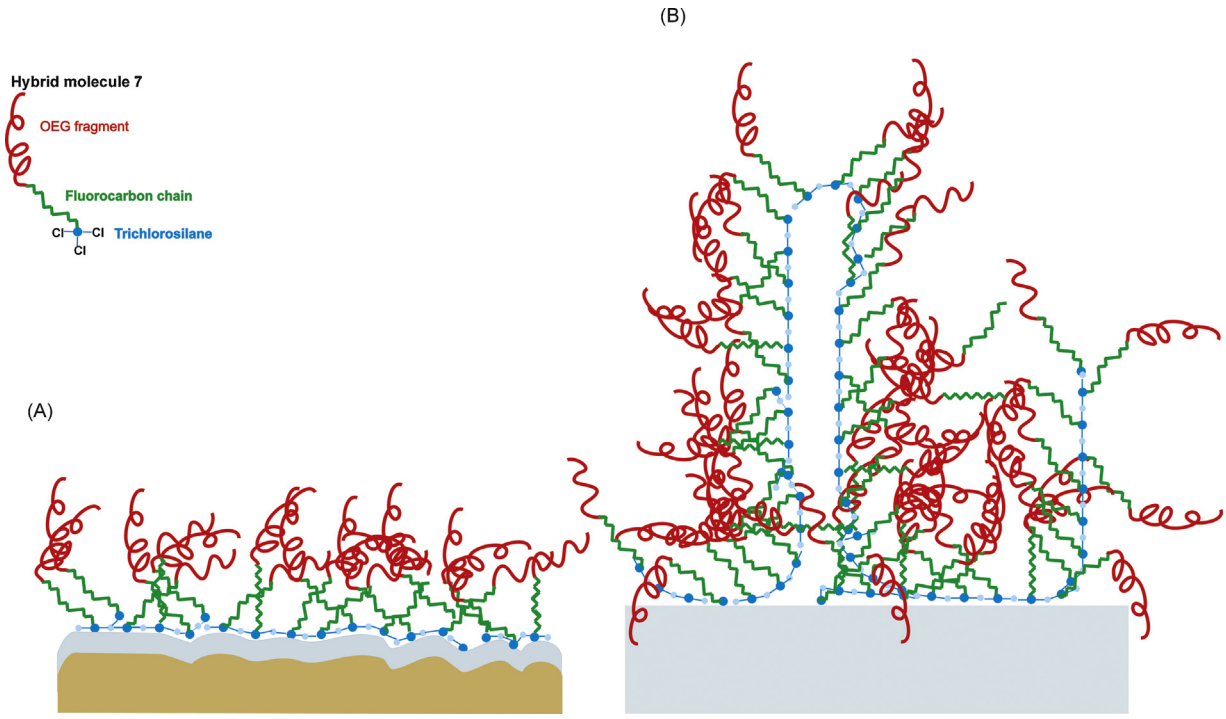

Scheme 3. Illustration of the packing of **7** in self-assembled films on (A) Au/SiO_x and (B) Si/SiO_x and BF33 surfaces.

4. Conclusions

In this paper the successful synthesis and monolayer properties of a new trichlorosilane **7** and dichlorosilane **8** are reported. Despite the fact that the reaction mixture contained the monomer (**7**) and the dimer (**8**), it was possible to form self-assembled films on various silica surfaces. The thickness, hydrophilicity and orientation of the hybrid compound **7** in self-assembled films depend on the nature of the used substrate. Scheme 3 shows schematically the molecular order in films of **7** self-assembled on Au/SiO_x surface as well as Si/SiO_x and BF33 surfaces.

SFM measurements of the film thickness indicated clearly that a monolayer of **7** was formed on the Au/SiO_x surface. Topography images as well as PM IRRAS showed that the monolayer was uniform and ordered at the molecular level as summarized in Scheme 3A. The OEG units exist in the amorphous phase. Long self-assembly times on the Au/SiO_x surface (>24 h) lead to some rearrangement in the monolayers, namely a transition of a small fraction of OEG chains from the amorphous state to the helical conformation was observed. In comparison to the thiol analogues, the hybrid molecule **7** formed less dense and less ordered monolayers. The long axis of the OEG fragment of the hybrid compound **7** tilts preferably parallel to the plane of the SiO_x surface. The anchoring $SiCl_3$ group is bulkier than the SH group adsorbing on the Au surface, therefore the expected packing density of silanes on the silica surface is lower than for thiols on gold. Interestingly, a new band at 1179 cm^{-1} appeared in the PM IRRA spectra of monolayers of **7** when self-assembly exceeded 24 h. This band is associated with the asymmetric stretching mode of Si—O—Si groups in the silica lattice of the monolayer. In silica films prepared via the sol-gel method it was observed at 1180 cm^{-1} [61]. Indeed, trichlorosilane groups of **7** may polymerize to form a lattice of silanes in the adsorbed film which lies parallel to the surface of the solid surface (Scheme 3A). This reaction may be responsible for the formation of well-defined pattern in the monolayers of **7** on the Au/SiO_x if self-assembly is carried out over realtively long times.

By contrast, the self-assembly of **7** on the Si/SiO_x and BF33 surfaces leads to the formation of films with poorly-defined packing and structure as shown in Scheme 3B. SFM measurements showed clearly that the self-assembled films of **7** on the Si/SiO_x and BF33 surfaces were inhomogenous and their thickness corresponded to length of 2–4 molecules of **7**. The process of adsorption is fast compared to the adsorption of **7** on Au/SiO_x. In this case the polymerization reaction of silanes seems to be responsible for a formation of disordered films. Interestingly, the chemisorption of **7** to the well-defined, almost atomically flat Si/SiO_x substrates is inefficient. This result suggests that the adsorbing molecules **7** and **8** require larger area than the distance between two anchor points on the silica lattice provides. The surface roughness of the Au/SiO_x substrate is significantly larger. The contained defects may provide sufficient space to accommodate a dense packing of **7** and formation of ordered monolayers. This is an important technological finding, which may facilitate controlling the order in the adsorbing monolayer via the control of the surface roughness of the silica surface. Initial tests of cell adhesion were done on silica **7** and **8** films modifying glass and silica surfaces. These results are shown in Supporting Information SI3.

Associated content

XPS survey spectra, changes of monolayer composition upon prolonged exposure to X-rays in UHV and cell seeding tests are available in Supporting Information.

Acknowledgements

We gratefully acknowledge Dr. Heiko Schramm (new address: Dynamit Nobel, Leverkusen, Germany) for preliminary synthetic studies and Prof. Dr. Monika Fritz (University of Bremen) for the introduction to contact mode AFM imaging in liquids. The authors would like to thank to Prof. Dr. Karl-Wilhelm Koch and Jutta Appelt (Carl von Ossietzky University of Oldenburg) for cell seeding tests

and taking of optical microscopy images. The project was funded by the Go-Bio initiative (FKZ 0315829) of the German Federal Ministry of Education and Research (BMBF).

References

[1] J.C. Love, L.A. Estroff, J.K. Kriebel, R.G. Nuzzo, G.M. Whitesides, Self-assembled monolayers of thiolates on metals as a form of nanotechnology, Chem. Rev. 105 (2005) 1103–1169.

[2] N. Herzer, S. Hoeppener, U.S. Schubert, Fabrication of patterned silane based self-assembled monolayers by photolithography and surface reactions on silicon-oxide substrates, Chem. Commun. 46 (2010) 5634–5652.

[3] S. Ciampi, J.B. Harper, J.J. Gooding, Wet chemical routes to the assembly of organic monolayers on silicon surfaces via the formation of Si–C bonds: surface preparation, passivation and functionalization, Chem. Soc. Rev. 39 (2010) 2158–2183.

[4] J.J. Gooding, S. Ciampi, The molecular level modification of surfaces: From self-assembled monolayers to complex molecular assemblies, Chem. Soc. Rev. 40 (2011) 2704–2718.

[5] S. Jiang, R. Frazier, E.S. Yamaguchi, M. Blanco, S. Dasgupta, Y. Tang, W.A. Goddard III, The SAM model for wear inhibitor performance of dithiophosphates on iron oxide, J. Phys. Chem. B 101 (1997) 7702–7709.

[6] A. Hozumi, B. Kim, T.J. McCarthy, Vapor-phase formation of alkyl isocyanate-derived self-assembled monolayers on titanium dioxide, Langmuir 25 (2009) 2875–2880.

[7] J.L. Wilbur, A. Kumar, H.A. Biebuyck, E. Kim, G.M. Whitesides, Microcontact printing of self-assembled monolayers: applications in microfabrication, Nanotechnology 7 (1996) 452–457.

[8] S. Xu, G.-y. Liu, Nanometer-scale fabrication by simultaneous nanoshaving and molecular self-assembly, Langmuir 13 (1997) 127–129.

[9] T. Wilhelm, G. Wittstock, Patterns of functional proteins formed by local electrochemical desorption of self-assembled monolayers, Electrochim. Acta 47 (2001) 275–281.

[10] R. Maoz, E. Frydman, S.R. Cohen, J. Sagiv, Constructive nanolithography: inert monolayers as patternable templates for in-situ nanofabrication of metal-semiconductor-organic surface structures. A generic approach, Adv. Mater. 12 (2000) 725–731.

[11] S.-Y. Ku, K.-T. Wong, A.J. Bard, Surface patterning with fluorescent molecules using click chemistry directed by scanning electrochemical microscopy, J. Am. Chem. Soc. 130 (2008) 2392–2393.

[12] M.N. Yousaf, B.T. Houseman, M. Mrksich, Using electroactive substrates to pattern the attachment of two different cell populations, Proc. Natl. Acad. Sci. USA 98 (2001) 5992–5996.

[13] R.-V. Ostaci, D. Damiron, Y. Grohens, L. Leger, E. Drockenmuller, Click chemistry grafting of Poly(ethylene glycol) brushes to alkyne-functionalized pseudobrushes, Langmuir 26 (2010) 1304–1310.

[14] C.C.A. Ng, S. Ciampi, J.B. Harper, J.J. Gooding, Antifouling behaviour of silicon surfaces modified with self-assembled monolayers containing both ethylene glycol and charged moieties, Surf. Sci. 604 (2010) 1388–1394.

[15] G. Elender, M. Kühner, E. Sackmann, Functionalization of Si/SiO_2 and glass surfaces with ultrathin dextran films and deposition of lipid bilayers, Biosens. Bioelectron. 11 (1996) 565–577.

[16] V. Atanasov, N. Knorr, R.S. Duran, S. Ingebrandt, A. Offenhäusser, W. Knoll, I. Köper, Membrane on a chip: a functional tethered lipid bilayer membrane on silicon oxide surfaces, Biophys. J. 89 (2005) 1780–1788.

[17] S. Prakash, T.M. Long, J.C. Selby, J.S. Moore, M.A. Shannon, Click modification of silica surfaces and glass microfluidic channels, Anal. Chem. 79 (2007) 1661–1667.

[18] T. Sordel, F. Kermarrec, Y. Sinquin, I. Fonteille, M. Labeau, F. Sauter-Starace, C. Pudda, F. de Crecy, F. Chatelain, M. De Waard, C. Arnoult, N. Picollet-D'hahan, The development of high quality seals for silicon patch-clamp chips, Biomaterials 31 (2010) 7398–7410.

[19] D.-H. Kim, D.-S. Shin, Y.-S. Lee, Spot arrays on modified glass surfaces for efficient SPOT synthesis and on-chip bioassay of peptides, J. Pept. Sci. 13 (2007) 625–633.

[20] A.N. Zelikin, B. Städler, Intelligent polymer thin films and coatings for drug delivery, in: H.M. Grandin, M. Textor (Eds.), Intelligent Surfaces in Biotechnology, 2012, pp. 243-290.

[21] H. Wang, J. Fang, T. Cheng, J. Ding, L. Qu, L. Dai, X. Wang, T. Lin, One-step coating of fluoro-containing silica nanoparticles for universal generation of surface superhydrophobicity, Chem. Commun. 87 (2008) 7–87, 9.

[22] R. Konradi, C. Acikgoz, M. Textor, Polyoxazolines for nonfouling surface coatings—a direct comparison to the gold standard PEG, Macromol. Rapid Commun. 33 (2012) 1663–1676.

[23] I. Banerjee, R.C. Pangule, R.S. Kane, Antifouling coatings recent developments in the design of surfaces that prevent fouling by proteins, bacteria, and marine organisms, Adv. Mater. 23 (2011) 690–718.

[24] R. Valiokas, S. Svedhem, M. Ostblom, S.C.T. Svensson, B. Liedberg, Influence of specific intermolecular interactions on the self-assembly and phase behavior of oligo(ethylene glycol)-terminated alkanethiols on gold, J. Phys. Chem. B 105 (2001) 5459–5469.

[25] M. Mrksich, G.M. Whitesides, Using self-assembled monolayers to understand the interactions of man-made surfaces with proteins and cells, Annu. Rev. Biophys. Biomol. Struct. 25 (1996) 55–78.

[26] L. Feuz, F. Höök, E. Reimhult, Design of intelligent surface modifications and optimal liquid handling for nanoscale bioanalytical sensors, in: H.M. Grandin, M. Textor (Eds.), Intelligent Surfaces in Biotechnology, 2012, pp. 71-122.

[27] K.L. Prime, G.M. Whitesides, Self-assembled organic monolayers: model systems for studying adsorption of proteins at surfaces, Science 252 (1991) 1164.

[28] S.-W. Lee, P.E. Laibinis, Protein-resistant coatings for glass and metal oxide surfaces derived from oligo(ethylene glycol)-terminated alkyltrichlorosilanes, Biomaterials 19 (1998) 1669–1675.

[29] C. Hoffmann, G.E.M. Tovar, Mixed self-assembled monolayers (SAMs) consisting of methoxy-tri(ethylene glycol)-terminated and alkyl-terminated dimethylchlorosilanes control the non-specific adsorption of proteins at oxidic surfaces, J. Colloid Interface Sci. 295 (2006) 427–435.

[30] S.S. Shah, M.C. Howland, L.-J. Chen, J. Silangcruz, S.V. Verkhoturov, E.A. Schweikert, A.N. Parikh, A. Revzin, Micropatterning of proteins and mammalian cells on indium tin oxide, ACS Appl. Mater. Interfaces 1 (2009) 2592–2601.

[31] A. Papra, N. Gadegaard, N.B. Larsen, Characterization of ultrathin Poly(ethylene glycol) monolayers on silicon substrates, Langmuir 17 (2001) 1457–1460.

[32] M. Cerruti, S. Fissolo, C. Carraro, C. Ricciardi, A. Majumdar, R. Maboudian, Poly(ethylene glycol) monolayer formation and stability on gold and silicon nitride substrates, Langmuir 24 (2008) 10646–10653.

[33] K.-H. Park, C. Berrier, F. Lebaupain, B. Pucci, J.-L. Popot, A. Ghazi, F. Zito, Fluorinated and hemifluorinated surfactants as alternatives to detergents for membrane protein cell-free synthesis, Biochem. J. 403 (2007) 183–187.

[34] J.G. Riess, Highly fluorinated amphiphilic molecules and self-assemblies with biomedical potential, Curr. Opin. Colloid Interface Sci. 14 (2009) 294–304.

[35] S.P. Pujari, E. Spruijt, M.A. Cohen Stuart, C.J.M. van Rijn, J.M.J. Paulusse, H. Zuilhof, Ultralow adhesion and friction of fluoro-hydro alkyne-derived self-assembled monolayers on h-terminated Si(1 1 1), Langmuir 28 (2012) 17690–17700.

[36] C. Gentilini, M. Boccalon, L. Pasquato, Straightforward synthesis of fluorinated amphiphilic thiols, Eur. J. Org. Chem. (2008) 3308–3313.

[37] C. Gentilini, F. Evangelista, P. Rudolf, P. Franchi, M. Lucarini, L. Pasquato, Water-soluble gold nanoparticles protected by fluorinated amphiphilic thiolates, J. Am. Chem. Soc. 130 (2008) 15678–15682.

[38] I. Zawisza, G. Wittstock, R. Boukherroub, S. Szunerits, PM IRRAS investigation of thin silica films deposited on gold. Part 1. Theory and proof of concept, Langmuir 23 (2007) 9303–9309.

[39] S. Szunerits, Y. Coffinier, S. Janel, R. Boukherroub, Stability of the gold/silica thin film interface: electrochemical and surface plasmon resonance studies, Langmuir 22 (2006) 10716–10722.

[40] J. Moulder, W.M. Stickle, P.E. Sobol, K.D. Bomben, Handbook of X-ray Photoelectron Spectroscopy, Physical Electronics, 1995.

[41] E. Liepins, I. Zicmane, E. Lukevics, A multinuclear NMR spectroscopy study of alkoxysilanes, J. Organomet. Chem. 306 (1986) 167–182.

[42] R.J. Klein, D.A. Fischer, J.L. Lenhart, Thermal and mechanical aging of self-assembled monolayers as studied by near edge X-ray absorption fine structure, Langmuir 27 (2011) 12423–12433.

[43] J. Genzer, E. Sivaniah, E.J. Kramer, J. Wang, M. Xiang, K. Char, C.K. Ober, R.A. Bubeck, D.A. Fischer, M. Graupe, R. Colorado Jr., O.E. Shmakova, T.R. Lee, Molecular orientation of single and two-armed monodendron semifluorinated chains on soft and hard surfaces studied using NEXAFS, Macromolecules 33 (2000) 6068–6077.

[44] S. Sambasivan, S. Hsieh, D.A. Fischer, S.M. Hsu, Effect of self-assembled monolayer film order on nanofriction, J. Vac. Sci. Technol. A 24 (2006) 1484–1488.

[45] J. Fréchette, R. Maboudian, C. Carraro, Thermal behavior of perfluoroalkylsiloxane monolayers on the oxidized Si(1 0 0) surface, Langmuir 22 (2006) 2726–2730.

[46] C.B. Kristalyn, S. Watt, S.A. Spanninga, R.A. Barnard, K. Nguyen, Z. Chen, Investigation of sub-monolayer, monolayer, and multilayer self-assembled semifluorinated alkylsilane films, J. Colloid Interface Sci. 353 (2011) 322–330.

[47] T. Miyazawa, K. Fukushima, Y. Ideguchi, Molecular vibrations and structure of high polymers. III. Polarized infrared spectrs, nomral vibrations, and helical conforamtion of polyethylene glycol, J. Chem. Phys. 37 (1962) 2764–2776.

[48] M. Himmelhaus, F. Eisert, M. Buck, M. Grunze, Self-assembly of *n*-alkanethiol monolayers. A study by IR-visible sum frequency spectroscopy (SFG), J. Phys. Chem. B 104 (2000) 576–584.

[49] I. Brand, M. Nullmeier, T. Klüner, R. Jogireddy, J. Christoffers, G. Wittstock, Structural analysis of $HS(CD_2)_{12}(O{-}CH_2{-}CH_2)_6OCH_3$ monolayers on gold by means of polarization modulation infrared reflection absorption spectroscopy. Progress of the reaction with bromine, Langmuir 26 (2010) 362–370.

[50] P. Harder, M. Grunze, R. Dahint, G.M. Whitesides, P.E. Laibinis, Molecular conformation in oligo(ethylene glycol)-terminated self-assembled monolayers on gold and silver surfaces determines their ability to resist protein adsorption, J. Phys. Chem. B 102 (1998) 426–436.

[51] C.T. Kirk, Quantitative analysis of the effect of disorder-induced mode coupling on infrared absorption in silica, Phys. Rev. B: Condens. Matter 38 (1988) 1255–1273.

[52] S. Herrwerth, W. Eck, S. Reinhardt, M. Grunze, Factors that determine the protein resistance of oligoether self-assembled monolayers—internal hydrophilicity, terminal hydrophilicity, and lateral packing density, J. Am. Chem. Soc. 125 (2003) 9359–9366.

[53] T.J. Lenk, V.M. Hallmark, C.L. Hoffmann, J.F. Rabolt, D.G. Castner, C. Erdelen, H. Ringsdorf, Structural investigation of molecular organization in self-assembled monolayers of a semifluorinated amidethiol, Langmuir 10 (1994) 4610–4617.
[54] S.L. Hsu, N. Reynolds, S.P. Bohan, H.L. Strauss, R.G. Snyder, Structure, crystallization, and infrared spectra of amorphous perfluoro-n-alkane films prepared by vapor condensation, Macromolecules 23 (1990) 4565–4575.
[55] C. Naselli, J.D. Swalen, J.F. Rabolt, Order-disorder transitions in Langmuir–Blodgett films. IV. Structure of cadmium bis[(11-perfluorooctyl)undecanoate] ($[F(CF_2)_8(CH_2)_{10}COO\text{-}]_2Cd_2+$) multilayers at ambient and elevated temperatures, J. Chem. Phys. 90 (1989) 3855–3860.
[56] M. Zaharescu, A. Jitianu, A. Braileanu, J. Madarasz, G. Pokol, Ageing effect on the SiO_2-based inorganic-organic hybrid materials, J. Therm. Anal. Calorim. 64 (2001) 689–696.
[57] B.C. Trasferetti, C.U. Davanzo, M.A. Bica de Moraes, LO–TO splittings in plasma-deposited siloxane films, J. Phys. Chem. B 107 (2003) 10699–10708.
[58] M.J. Pellerite, E.J. Wood, V.W. Jones, Dynamic contact angle studies of self-assembled thin films from fluorinated alkyltrichlorosilanes, J. Phys. Chem. B 106 (2002) 4746–4754.
[59] B.C. Bunker, R.W. Carpick, R.A. Assink, M.L. Thomas, M.G. Hankins, J.A. Voigt, D. Sipola, M.P. de Boer, G.L. Gulley, The impact of solution agglomeration on the deposition of self-assembled monolayers, Langmuir 16 (2000) 7742–7751.
[60] G. Tizazu, O. El Zubir, S. Patole, A. McLaren, C. Vasilev, D.J. Mothersole, A. Adawi, C.N. Hunter, D.G. Lidzey, G.P. Lopez, G.J. Leggett, Micrometer and nanometer scale photopatterning of proteins on glass surfaces by photo-degradation of films formed from oligo(ethylene glycol) terminated silanes, Biointerphases 7 (2012) 54.
[61] J. Niedziolka, B. Palys, R. Nowakowski, M. Opallo, Characterization of gold electrodes modified with methyltrimethoxysilane and (3-mercaptopropyl)trimethoxysilane sol–gel processed films, J. Electroanal. Chem. 578 (2005) 239–245.